AD-A072 083 NATIONAL AVIATION FACILITIES EXPERIMENTAL CENTER ATL--ETC F/G 17/9
CALCULATION OF THE CORRELATION REGION SIZE FOR USE WITH ALPHA-B--ETC(U)
APR 79 R E LEFFERTS

UNCLASSIFIED FAA-NA-79-15 NL

| OF |
AD
A072083

END
DATE
FILMED
9-79
DDC

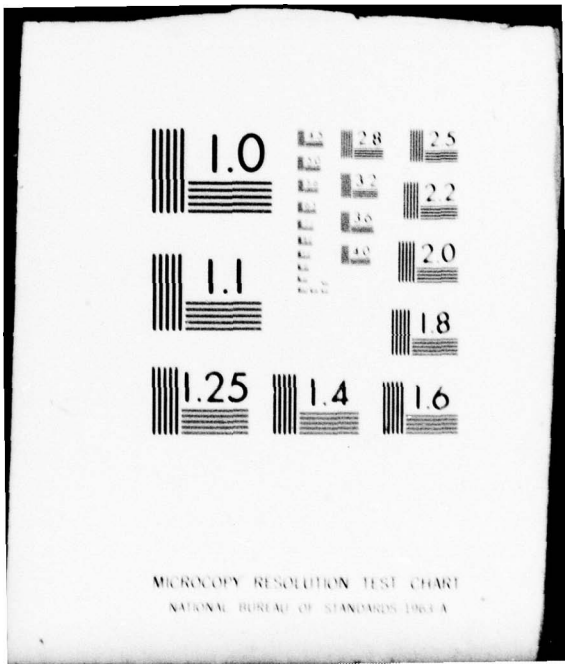
1.0
1.1
1.25
1.4
1.6
2.8
3.2
3.6
4.0
2.5
2.2
2.0
1.8
MICROCOPY RESOLUTION TEST CHART
NATIONAL BUREAU OF STANDARDS 1963-A

Report No. FAA-NA-79-15

LEVEL II

12 B-S

CALCULATION OF THE CORRELATION REGION SIZE FOR USE WITH ALPHA-BETA TRACKING FILTERS

Robert E. Lefferts

APRIL 1979

NAFEC REPORT

Document is available to the U.S. public through the National Technical Information Service, Springfield, Virginia 22161.

Prepared for

U.S. DEPARTMENT OF TRANSPORTATION
FEDERAL AVIATION ADMINISTRATION
National Aviation Facilities Experimental Center
Atlantic City, New Jersey 08405

NOTICE

The United States Government does not endorse products or manufacturers. Trade or manufacturer's names appear herein solely because they are considered essential to the object of this report.

Technical Report Documentation Page

1. Report No.	2. Government Accession No.	3. Recipient's Catalog No.
FAA-NA-79-15		

4. Title and Subtitle
CALCULATION OF THE CORRELATION REGION SIZE FOR USE WITH ALPHA-BETA TRACKING FILTERS

5. Report Date
Apr 1979

6. Performing Organization Code
ANA-220

7. Author(s)
Robert E. Lefferts

8. Performing Organization Report No.
FAA-NA-79-15

9. Performing Organization Name and Address
Federal Aviation Administration
National Aviation Facilities Experimental Center
Atlantic City, New Jersey 08405

10. Work Unit No. (TRAIS)

11. Contract or Grant No.
975-200-10A

12. Sponsoring Agency Name and Address
Federal Aviation Administration
National Aviation Facilities Experimental Center
Atlantic City, New Jersey 08405
31 p.

13. Type of Report and Period Covered
NAFEC

14. Sponsoring Agency Code
ANA-1

15. Supplementary Notes
Tracking performance is discussed in report FAA-NA-79-16

ALPHA BETA

A072054

16. Abstract

The design of correlation regions for tracking with cooperative users is examined under the requirement to design the correlation regions on a constant probability of intercept basis. Starting with the assumption of independent and Gaussian-distributed range and azimuth errors in the sensor and assuming a constant-coefficient isotropic α-β tracking filter, it is shown how the correlation region design must include such factors as sensor errors, timing jitter, tracking errors, and the asynchronous operation of the tracking function with respect to the sensor measurements. Using a specific example to obtain numerical results, it is shown that, in the case of straight-line trajectories, the radius of a circular correlation region is linearly proportional to the distance from the sensor in the region where azimuthal errors predominate and is constant in the region where range errors predominate. For a maneuvering target, it is shown that the size of the correlation region must be equal to the sum of the radius used for the straight-line case plus the magnitude of any tracking bias which results because of the deviation from a straight-line trajectory as assumed in the tracking filter. By examining various types of maneuvers, an upper bound is derived for the magnitude of the bias which could reasonably be expected in typical maneuvers. By specifying the size of the correlation region on a constant probability bias, it should be possible to obtain better discrimination against false targets and improved detection of maneuvers by sensing the development of tracking biases.

17. Key Words		18. Distribution Statement
Tracking	Correlation Regions	Document is available to the U.S. Public through National Technical Information Service, Springfield, Virginia, 22161
α-β Filters	Search Radar	
Radar Tracking		
Track-while-scan radars		

19. Security Classif. (of this report)	20. Security Classif. (of this page)	21. No. of Pages	22. Price
Unclassified	Unclassified	30	

Form DOT F 1700.7 (8-72) Reproduction of completed page authorized

240 550

METRIC CONVERSION FACTORS

Approximate Conversions to Metric Measures

Symbol	When You Know	Multiply by	To Find	Symbol
	LENGTH			
in	inches	*2.5	centimeters	cm
ft	feet	30	centimeters	cm
yd	yards	0.9	meters	m
mi	miles	1.6	kilometers	km
	AREA			
in^2	square inches	6.5	square centimeters	cm^2
ft^2	square feet	0.09	square meters	m^2
yd^2	square yards	0.8	square meters	m^2
mi^2	square miles	2.6	square kilometers	km^2
	acres	0.4	hectares	ha
	MASS (weight)			
oz	ounces	28	grams	g
lb	pounds	0.45	kilograms	kg
	short tons (2000 lb)	0.9	tonnes	t
	VOLUME			
tsp	teaspoons	5	milliliters	ml
Tbsp	tablespoons	15	milliliters	ml
fl oz	fluid ounces	30	milliliters	ml
c	cups	0.24	liters	l
pt	pints	0.47	liters	l
qt	quarts	0.95	liters	l
gal	gallons	3.8	liters	l
ft^3	cubic feet	0.03	cubic meters	m^3
yd^3	cubic yards	0.76	cubic meters	m^3
	TEMPERATURE (exact)			
°F	Fahrenheit temperature	5/9 (after subtracting 32)	Celsius temperature	°C

*1 in = 2.54 (exactly). For other exact conversions and more detailed tables, see NBS Misc. Publ. 286, Units of Weights and Measures, Price $2.25, SD Catalog No. C13.10:286.

Approximate Conversions from Metric Measures

Symbol	When You Know	Multiply by	To Find	Symbol
	LENGTH			
mm	millimeters	0.04	inches	in
cm	centimeters	0.4	inches	in
m	meters	3.3	feet	ft
m	meters	1.1	yards	yd
km	kilometers	0.6	miles	mi
	AREA			
cm^2	square centimeters	0.16	square inches	in^2
m^2	square meters	1.2	square yards	yd^2
km^2	square kilometers	0.4	square miles	mi^2
ha	hectares (10,000 m^2)	2.5	acres	
	MASS (weight)			
g	grams	0.035	ounces	oz
kg	kilograms	2.2	pounds	lb
t	tonnes (1000 kg)	1.1	short tons	
	VOLUME			
ml	milliliters	0.03	fluid ounces	fl oz
l	liters	2.1	pints	pt
l	liters	1.06	quarts	qt
l	liters	0.26	gallons	gal
m^3	cubic meters	35	cubic feet	ft^3
m^3	cubic meters	1.3	cubic yards	yd^3
	TEMPERATURE (exact)			
°C	Celsius temperature	9/5 (then add 32)	Fahrenheit temperature	°F

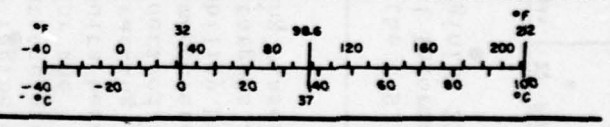

TABLE OF CONTENTS

LIST OF ILLUSTRATIONS

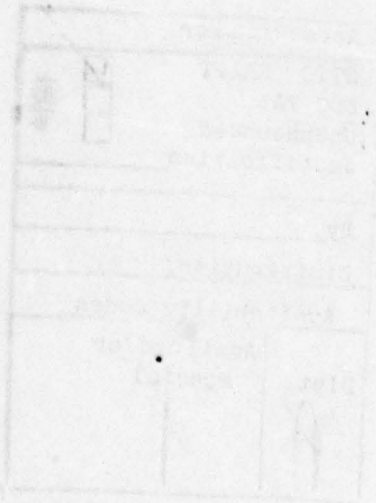

EXECUTIVE SUMMARY

The basis for all advanced air traffic control functions is the ability to predict the position of an aircraft sufficiently far into the future to allow intervention by a controller in situations in which this is warranted. The prediction of future position is based on velocity estimates obtained from a tracking filter which estimates, via numerical differentiation, the time derivatives of the position reports for a given aircraft. Within the tracking algorithm, the correlation region, or search area, is one of the means by which new target reports are associated with existing tracks derived from previous reports. The topic of interest in this paper is the design of search areas which will achieve a high level of correct association between the existing tracks and new target reports, but which are sufficiently selective to reject erroneous reports such as false targets. In order to achieve this goal it is necessary to design search areas which are adaptive to the statistical performance throughout the coverage area of the sensor.

The design of variable or dynamic search areas is based on both the measurement errors of the sensor and the performance of the tracking filter for various types of maneuvers. In all practical tracking algorithms the trajectories of maneuvering targets are more difficult to follow than straight-line tracks. Since the size of the dynamic search area varies with the size of the expected measurement error, and other factors, this technique is able to provide a better discrimination between straight-line and maneuvering targets which results in an improvement of the tracking performance (via a reduction in the bias observed in heading for maneuvers and a reduction in the heading jitter for straight-line tracks). Since the search area design is based on known statistical characteristics of the sensor measurement errors, the theoretical performance of the tracking algorithm and the deviations from the theoretical performance encountered in practical tracking algorithms, the dynamic search area concept guarantees that a specified level of tracking performance will be maintained throughout the coverage area of the sensor. The numerical techniques developed in this paper are applicable to the design of dynamic search areas for use with tracking filters using either DABS or ATCRBS data. In a subsequent paper, the specific levels of tracking performance improvement which can be obtained using the dynamic search area will be found.

1. INTRODUCTION

The process of radar data correlation, which is defined as the association of surveillance data with a track (a mathematical estimation of a target trajectory), has been considered previously [1-7]. The requirement for a correlation process usually arises in the transfer of tracking responsibility between surveillance volumes covered by different sensors or in the multiple-target/multiple-sensor case for the same surveillance volume where an association between tracking and surveillance data, which may contain false reports, must be made. In most cases the size of the gate (or search area) in which correlation will be allowed is based on the statistical properties of the residual errors between the measured target data and the predicted state of the trajectory at the time of interest. If it is assumed that the distribution of the residuals is Gaussian and independent in each dimension, then the gate boundary will usually be taken as an equiprobability contour with the statistical properties based on the chi-square distribution [3, 5, and 7].

The usual context for correlation analyses is in the case of uncooperative users in which there is a noise background of spurious data combined with true target reports corrupted by measurement errors. For the purpose of this study, however, it will be assumed that cooperative targets (i.e., transponder equipped) are being observed and for this the correlation problem is of a slightly different nature. The system of interest in this case is the Air Traffic Control Radar Beacon System (ATCRBS) [8] in which the correlation process is used to reject data which are unreasonable because of inherent system limitations (e.g., identification errors in the beacon code reply can be caused by overlapping replies from closely spaced targets, erroneous positions can be reported due to reflections, etc.). In addition to rejecting unreasonable data, the correlation process must also determine which of several alternative data points, if any exist, is the best for a particular track and, also, to detect a target maneuver by the size of the residual error. It has been suggested that data association and tracking should be treated in a unified manner rather than relying on simulation of alternative techniques [1], and it is the objective in this study to illustrate the interrelationship between correlation and tracking and to show how certain practical problems of implementation can affect the design.

2. MATHEMATICAL DEVELOPMENT

2.1 SURVEILLANCE MODEL.

In order to make probabilistic statements about the size of the correlation regions, some form of statistical model must be used to describe the sensor measurement process. It will be assumed, as it has been in other studies [20], that the surveillance system measures target position in a polar

coordinate system and that the range and azimuth errors are small in magnitude, Gaussian distributed, and statistically independent. The transformation to the Cartesian coordinate system used for tracking is, where θ is measured from the y-axis,

$$x = \rho \sin \theta \tag{1}$$

$$y = \rho \cos \theta \tag{2}$$

and for small errors a first-order approximation is

$$\Delta x = \sin \theta \ \Delta \rho + \rho \cos \theta \ \Delta \theta \tag{3}$$

$$\Delta y = \cos \theta \ \Delta \rho - \rho \sin \theta \ \Delta \theta . \tag{4}$$

It is implicitly assumed in the above transformation that data from targets at different altitudes have been mapped onto a common plane using an appropriate projection technique. Assuming that the errors in range and azimuth are unbiased then Δx and Δy are bivariate Gaussian random variables with zero mean and variances

$$\sigma_x^2 = \sin^2 \theta \ \sigma_\rho^2 + (\rho \cos \theta)^2 \ \sigma_\theta^2 \tag{5}$$

$$\sigma_y^2 = \cos^2 \theta \ \sigma_\rho^2 + (\rho \sin \theta)^2 \ \sigma_\theta^2 \tag{6}$$

$$\sigma_{xy} = (\sigma_\rho^2 - \rho^2 \sigma_\theta^2) \ \sin \theta \cos \theta . \tag{7}$$

Equations (3) and (4) can be solved simultaneously for $\Delta\rho$ and $\Delta\theta$, and the resulting equations can be used to express the variances in a polar coordinate system in terms of the variances in a Cartesian coordinate system; i.e.,

$$\sigma_\rho^2 = \sigma_x^2 \sin^2 \theta + \sigma_y^2 \cos^2 \theta + 2\sigma_{xy} \sin \theta \cos \theta \tag{8}$$

$$\sigma_\theta^2 = (\sigma_x^2 \cos^2 \theta + \sigma_y^2 \sin^2 \theta - 2\sigma_{xy} \sin \theta \cos \theta)/\rho^2 . \tag{9}$$

While (8) and (9) are valid for any Gaussian distribution, it will not necessarily be true that ρ and θ are statistically independent. If, however, the statistical characteristics in the Cartesian coordinate system were originally derived from a polar coordinate system, via (5) to (7), then ρ and θ, in a

a polar coordinate system with statistical characteristics defined by (8) and (9), will be statistically independent. The usefulness of the transformation from a polar to a Cartesian coordinate system and subsequently reverting to a polar coordinate system will become apparent in a later section in which the evaluation of certain integrals is discussed.

2.2 SPECIFICATION OF THE TRACKING FILTER.

The sensor measurements consist of the sequences $\{\rho(k)\}$ and $\{\theta(k)\}$ where $\rho(k)$ and $\theta(k)$ are the true range and azimuth, respectively, of the target at time epoch k. In practice, the sensor measurements are corrupted by errors, $\Delta\rho(k)$ and $\Delta\theta(k)$, and it will be assumed that the sequences $\{\Delta\rho(k)\}$ and $\{\Delta\theta(k)\}$ are each white and stochastically independent of one another. After transformation to a Cartesian coordinate system via (1) and (2), the measurement sequences $\{X_m(k)\}$ and $\{Y_m(k)\}$ with the associated error sequences as defined by (3) and (4) are input to a digital filter which is characterized by the recursive equations,

$$X_s(k) = X_p(k) + \alpha\,(X_m(k) - X_p(k)) \tag{10}$$

$$V_s(k) = V_s(k-1) + (\beta/T)\;\;(X_m(k) - X_p(k)) \tag{11}$$

$$X_p(k+1) = X_s(k) + T\,V_s(k) \tag{12}$$

where X_s, V_s, X_p are the smoothed position, smoothed velocity, and predicted position, respectively, and similarly for Y. The sensor data, X_m, are assumed to be available at a constant rate specified by the time interval T. The properties of this filter, known as an α-β filter, are well known [9-24]. The usefulness of this filter, as compared to others with superior performance, lies mainly in its ease of implementation and limited computational requirements which allows tracking of large numbers of targets with computers of relatively modest capacity. The smoothing constants α and β determine the performance of the tracking filter and various criteria have been developed for specifying these constants [9-13]. Smaller smoothing constants generally give better noise reduction properties, while larger smoothing constants give better transient or maneuver-following capability. Since it is not possible to select smoothing constants which are optimal in all cases, it is frequently necessary to use several sets of smoothing constants to achieve a practical system. The choice between sets of smoothing constants is then based on the magnitude of the difference between the measured position and the predicted position which is referred to as the track datum deviation.

In the analysis of the α-β tracking filter, it is normally assumed that the filter operates at a constant rate with data available at the same rate. While this is a reasonable assumption in the case of a single sensor, in the case of multiple sensors, each of which covers only a portion of the total surveillance volume, it is unlikely that the sensor system and the tracking system will operate in a synchronous manner so that the time of receipt of the data may not be the same as the prediction time of the tracking system. Such a situation arises in the enroute air traffic control system in which the

smoothing and prediction process is done at fixed intervals which are asynchronous with respect to the sampling intervals of the sensors (in fact, the sampling intervals of the sensors are not all the same). To compensate for the asynchronous operation of the tracking and sensor systems, the estimated velocity is used to shift the measured position in time so as to be time coincident with the predicted position, thus attempting to duplicate the operation of a synchronous sensor/tracking system. In this case, (10) and (11) become

$$X_s(k) = X_p(k) + \alpha\,(X_m(k) + \Delta T_c(k)\, V_s(k-1) - X_p(k)) \tag{13}$$

$$V_s(k) = V_s(k-1) + (\beta/T)\,(X_m(k) + \Delta T_c(k)\, V_s(k-1) - X_p(k)) \tag{14}$$

where ΔT_c is the difference between the time of receipt of $X_m(k)$ and the time used in the calculation of the predicted position $X_p(k)$. The requirement to adjust the smoothing and prediction process to account for the time of actual receipt of the datum has been recognized along with the fact that the gate size must be, "...large enough to account for all sources of error" [10] in order to achieve correlation with the target data.

The fact that a 'time-correction' process must be used to compensate for the asynchronous operation of the tracking algorithm implies that the correlation process must be a two-stage procedure, since the process of time correction itself implies that at least a tentative correlation has already been made, unless, of course, an exhaustive search is made considering every possible track-datum pairing. Many techniques have been developed for making tentative correlations and these include: (a) associating the beacon code of the datum with the code of a track which already exists, (b) dividing the surveillance volume into subvolumes with lists of the tracks in each subvolume, and (c) the use of a preliminary search area defined, for example, as

$$|X_m(k) - X_p(k)| \leq D \tag{15}$$

$$|Y_m(k) - Y_p(k)| \leq D \tag{16}$$

where D is chosen large enough to include all possible track-datum pairings which might be allowable in the second stage of correlation. It will be assumed that some technique is available to make tentative correlations, similar to the coarse/fine correlation in [3] or one of the techniques above, so that it is not necessary to make exhaustive search of every possible track-datum pairing. Regardless of which technique is used the characteristics are the same, namely that the preliminary or coarse stage must process large amounts of data with very low computational requirements for each pairing, while the second or "fine" stage processes small amounts of data, but may have considerably higher computational requirements for each pairing.

2.3 TRACK DATUM DEVIATION.

In the second or fine stage of the correlation process, which is of primary interest in this study, some means must be available to assess the quality the various track/datum pairings which result from the tentative correlatio made in the first stage of the correlation process. Assuming that all other relevant factors are equal the best track/datum pairing will be that which minimizes the magnitude of the track datum deviation, $\Delta\vec{r}$, which is given by (including the time-correction factor),

$$\Delta\vec{r}(k) = \vec{r}_m(k) + \Delta T_c(k)\vec{V}_s(k-1) - \vec{r}_p(k) \tag{17}$$

where $\vec{r}_m$, $\vec{V}_s$, and $\vec{r}_p$ are the measured position, smoothed velocity, and predicted position, respectively, and it is now explicitly denoted that the track datum deviation is a vector as are the positions and velocity. Since $|\Delta\vec{r}(k)|$ will be used as the final basis for correlation, the statistical characteristics of $\Delta\vec{r}(k)$ must be determined to know how large a deviation is reasonable. Expressing each of the terms in (17) as the sum of a true component plus a random error yields (where, for simplicity, the dependence on k has been assumed),

$$\Delta\vec{r} = \vec{r}_{T_1} + \vec{r}_{e_1} + (\Delta T_T + \epsilon)\,(\vec{V}_T + \vec{V}_e) - \vec{r}_{T_2} - \vec{r}_{e_2} \tag{18}$$

or

$$\Delta\vec{r} = \vec{r}_{T_1} + \Delta T_T\vec{V}_T - \vec{r}_{T_2} + \vec{r}_{e_1} + \epsilon\vec{V}_T + \Delta T_T\vec{V}_e + \epsilon\vec{V}_e - \vec{r}_{e_2} \tag{19}$$

where ϵ is a timing error which arises from the fact that time is measured in discrete increments. Of course, in a digital computer all data are quantized but the additional errors introduced by finite precision computations will be assumed to be negligible. If the trajectory dynamics implied by (12), i.e., a constant velocity straight-line path, are, in fact, correct, then the first three terms of (19) will vanish since $T_1 + T_T = T_2$. If the target is maneuvering, however, there will be a bias error introduced in $\Delta\vec{r}$ by the fact that the assumed system model is not correct. For the present, however, it will be assumed that the system model is correct so that (19) becomes

$$\Delta\vec{r} = \vec{r}_{e_1} + \epsilon\vec{V}_T + T_T\vec{V}_e + \epsilon\vec{V}_e - \vec{r}_{e_2} \tag{20}$$

in which the statistical properties of $\vec{r}_{e_1}$ are given by (5)-(7). In the case of the timing error, ϵ, it will be assumed that these errors are uniformly distributed over an interval ΔT_q with $E(\epsilon)=0$, which can easily be obtained by an appropriate choice of the time origin, so that for $\epsilon\vec{V}_T$,

$$\sigma_{qx}^2 = \sigma_q^2 V_x^2 \tag{21}$$

$$\sigma_{qy}^2 = \sigma_q^2 V_y^2 \tag{22}$$

$$\sigma_{qxy} = \sigma_q^2 V_x V_y \tag{23}$$

where

$$\sigma_q^2 = (\Delta T_q)^2/12 \tag{24}$$

and V_x and V_y are the components of the true velocity.

2.4 STATISTICAL PERFORMANCE OF THE $\alpha - \beta$ TRACKING FILTER.

The statistical properties of the last three terms in (20) depend on the noise reduction performance of the tracking filter. The tracking filter (in both dimensions) can be considered as a single-input (X_m), multiple output (X_s, V_s, X_p) filter which can be shown to have unbiased outputs if X_m is unbiased, as it is in this case (this is also true in the case where time-correction is used). Therefore, the statistical characteristics of a constant coefficient, isotropic $\alpha - \beta$ tracking filter are completely expressed in terms of the normalized variance reduction ratios,

$$\sigma_s^2 = K_s \sigma_x^2 \tag{25}$$

$$\sigma_v^2 = K_v \sigma_x^2 \tag{26}$$

$$\sigma_p^2 = K_p \sigma_x^2 \tag{27}$$

where K_s, K_v, and K_p are the reduction ratios for X_s, V_s, and X_p, respectively, and σ_x^2 is the variance of the noise at the input of the filter. Expressed in terms of the smoothing constants, the variance reduction ratios are [11, 23],

$$K_s = \frac{2\alpha^2 + \beta(2-3\alpha)}{\alpha(4-2\alpha-\beta)} \tag{28}$$

$$K_v = \frac{1}{T^2} \frac{2\beta^2}{\alpha(4-2\alpha-\beta)} \tag{29}$$

$$K_p = \frac{2\alpha^2 + \alpha\beta + 2\beta}{\alpha(4-2\alpha-\beta)} \tag{30}$$

where T is the constant smoothing interval.

The variance reduction ratios, however, do not include the effects of time-correction which is simply a feedback loop, as shown in Figure 1, in which there is an additional noise source to account for time quantization in the time-correction process. Since the errors are additive and statistically independent

$$\sigma^2_{\hat{x}} = \sigma^2_x + \sigma^2_q \; V^2_x \tag{31}$$

so that the variance at the input to the filter in which time-correction is used is $\sigma^2_{\hat{x}}$.

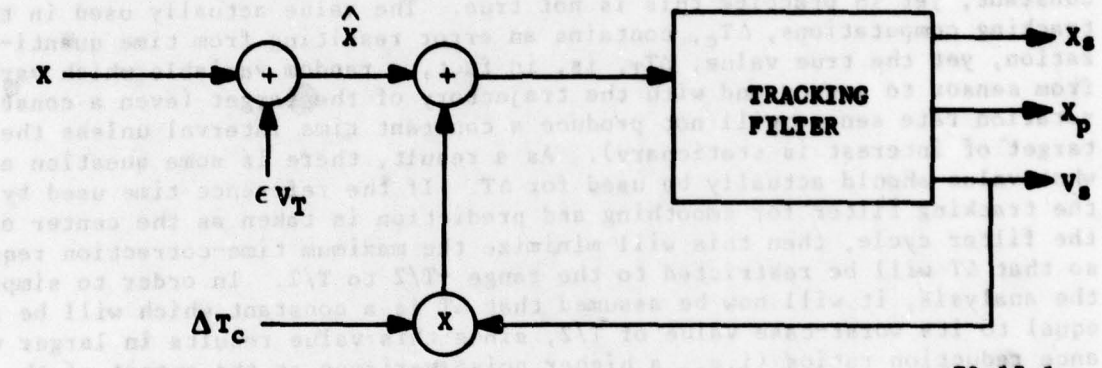

FIGURE 1. FEEDBACK LOOP ILLUSTRATING TIME CORRECTION AND TIME QUANTIZATION ERRORS

Since the introduction of time-correction would be expected to modify the noise rejection performance of the tracking filter, the variance reduction ratios for the case where time-correction is used were calculated using the standard z-transform method [24], and for this case

$$K_s = (2\alpha^2 - 3\alpha\beta + 2\beta + \beta^2 \, \Delta T/T)/\Delta \tag{32}$$

$$K_v = 2(\beta/T)^2/\Delta \tag{33}$$

$$K_p = (2\alpha^2 + \alpha\beta + 2\beta + \beta^2 \Delta T/T)/\Delta \tag{34}$$

where $\Delta = \alpha(4-2\alpha-\beta) - \beta(4-4\alpha-\beta)\Delta T/T - 2(\beta\Delta T/T)^2$ (35)

which reduce to the results given previously when $\Delta T=0$. The variance reduction ratios can also be derived using a matrix approach [21, 22].

Since the three filter outputs are obtained from a common input, X_m, it would be expected that a nonzero correlation would exist between the various outputs so an additional item of interest, which will be required to determine the statistical characteristics of $\Delta\vec{r}$, is the covariance between the velocity and the smoothed position which is given by the normalized covariance ratio,

$$K_{vs} = \beta(2\alpha-\beta)/(T\Delta). \quad (36)$$

In the derivation of the above equations, it was assumed that ΔT was a known constant, yet in practice this is not true. The value actually used in the tracking computations, ΔT_c, contains an error resulting from time quantization, yet the true value, ΔT_T, is, in fact, a random variable which varies from sensor to sensor and with the trajectory of the target (even a constant rotation rate sensor will not produce a constant time interval unless the target of interest is stationary). As a result, there is some question as to what value should actually be used for ΔT. If the reference time used by the tracking filter for smoothing and prediction is taken as the center of the filter cycle, then this will minimize the maximum time-correction required so that ΔT will be restricted to the range $-T/2$ to $T/2$. In order to simplify the analysis, it will now be assumed that ΔT is a constant which will be set equal to its worst-case value of $T/2$, since this value results in larger variance reduction ratios (i.e., a higher noise variance at the output of the filter). As a result of this assumption the statistical properties of all terms in (20) are now known with the exception of $\epsilon\vec{V}_e$.

The probability density function for the product term, $\epsilon\vec{V}_e$, can be shown to be an exponential integral, but since these random variables are independent with mean zero, the variance of the product is simply the product of the variances. In this case, the variances of the last three terms in (20) can be obtained from the variance reduction ratios applied to $\sigma^2_{\hat{x}}$ so that, noting that $\vec{V}_e$ and $\vec{r}_{e_2}$ are not independent,

$$\sigma^2_{xr} = (\sigma^2_x + V^2_x\ \sigma^2_q)\ (1 + (\Delta T^2\ + \sigma^2_q)\ K_v + K_p \quad (37)$$
$$-2\Delta T\ (K_{vs} + TK_v))$$

where σ^2_{xr} is the variance of the x-component of $\Delta\vec{r}$ and similarly for σ^2_{yr} and σ_{xyr}. It is implicitly assumed in (37) that the scan-to-scan differences in the statistical properties of σ^2_x (and σ^2_y, σ_{xy} also) are negligible which

is a reasonable assumption except at points close to the radar where the range to the target may be on the same order of magnitude as the distance moved by the target in the smoothing interval T. The probability for any particular search area of interest, including the effects of tracking and time-correction, can, therefore, be obtained by integrating the bivariate Gaussian distribution, defined by σ^2_{xr}, σ^2_{yr}, and σ_{xyr}, over the region of interest.

The value of the integral just defined will be the probability of a successful fine correlation when the search area for $\Delta\vec{r}$ is the same as the area over which the integration is performed. The use of the Gaussian distribution requires the implicit assumption that the sensor measurement errors are significantly larger than the errors introduced by finite precision computations and time and signal quantization which will be the case in a well-designed system.

3. NUMERICAL RESULTS FOR CIRCULAR SEARCH AREAS

For the purposes of this study circular search areas will be used even though the track datum deviation density assumes a highly elliptical shape as the range to the target increases (resulting from the predominance of azimuthal errors at large distances). The circular search area has a significant practical advantage in that the correlation decision can be based solely on the magnitude of the track datum deviation, $|\Delta\vec{r}|$, or the square of the magnitude in order to avoid a square-root computation, and the angular relationship between the datum and the track can be ignored. Thus, the circular search area has a considerable computational advantage over noncircular search areas which would impose a much higher computational burden. The design of the search area is now reduced to the problem of determining the maximum value of the track datum deviation for which correlation will be allowed. Since it is desirable to maintain the same level of tracking performance throughout the entire coverage region, the size of the search area must be a function of the range from the sensor to compensate for the increasing significance of azimuthal errors. Acceptable tracking performance requires a high degree of correlation so that the search area must be large enough to include a significant portion of the region in which the desired data point might be found. To design search areas to have a constant probability of intercept, say 95 percent, it is necessary to integrate the bivariate Gaussian distribution over a circular region and to present these results, in terms of the radius of the circle, as a function of the distance to the sensor, which will achieve the desired level of correlation. To simplify the numerical computations required, it would be desirable to reduce the two-dimensional integral to a single dimensional integral, and three means have been found by which this can be accomplished.

3.1 EVALUATION BY DIRECT INTEGRATION OF f(r).

The magnitude, r, of the radius vector for a correlated bivariate Gaussian distribution with zero mean is given by the Nakagami q-distribution [25,26]:

$$f(r) = \frac{2r}{\sqrt{ab}} \exp\left[-\frac{r^2}{2}\left(\frac{1}{a} + \frac{1}{b}\right)\right] I_o\left(\frac{r^2}{2}\left(\frac{1}{b} - \frac{1}{a}\right)\right) \tag{38}$$

where

$$a = \sigma_x^2 + \sigma_y^2 + \sqrt{(\sigma_y^2 - \sigma_x^2)^2 + (2c\sigma_x \sigma_y)^2} \tag{39}$$

$$b = \sigma_x^2 + \sigma_y^2 - \sqrt{(\sigma_y^2 - \sigma_x^2)^2 + (2c\sigma_x \sigma_y)^2} \tag{40}$$

$$c = \sigma_{xy} / \sigma_x \sigma_y \tag{41}$$

and $I_o(\cdot)$ is the modified Bessel function of the first kind with order zero (which is easily calculated; e.g., [27, 28]). The required probability, using (37) to calculate the variances for (39)-(41), is

$$P(R) = \int_0^R f(r)\, dr \tag{42}$$

which can be obtained using one of the many numerical techniques for evaluating single dimensional integrals (e.g., Gaussian quadrature [27, 29] was used in this study).

3.2 EVALUATION IN POLAR COORDINATES.

Since the range and azimuth errors are assumed to be independent, equations (8) and (9) can be applied using (37), assuming that the time-quantization errors are insignificant, to revert to a polar coordinate system in which the variables of the joint density function are separable. The limits on the range integration as a function of azimuth can be determined from the Law of Cosines (see Figure 2):

$$r_{max} = \rho \cos\theta + \sqrt{R^2 - (\rho \sin\theta)^2} \tag{43}$$

$$r_{min} = \rho \cos\theta - \sqrt{R^2 - (\rho \sin\theta)^2} \tag{44}$$

then, expressing the integral over range in terms of the error function [26] and noting the symmetry in azimuth,

$$P(R) = \int_0^{\sin^{-1}(R/\rho)} \{\mathrm{erf}((r_{max}-\rho)/\sqrt{2}\sigma_\rho) - \mathrm{erf}((r_{min}-\rho)/\sqrt{2}\sigma_\rho)\} \frac{\exp(-\theta^2/2\sigma_\theta^2)}{\sqrt{2\pi}\,\sigma_\theta}\, d\theta \qquad (45)$$

which can also be evaluated using Gaussian quadrature and where erf(·) is the standard error function integral.

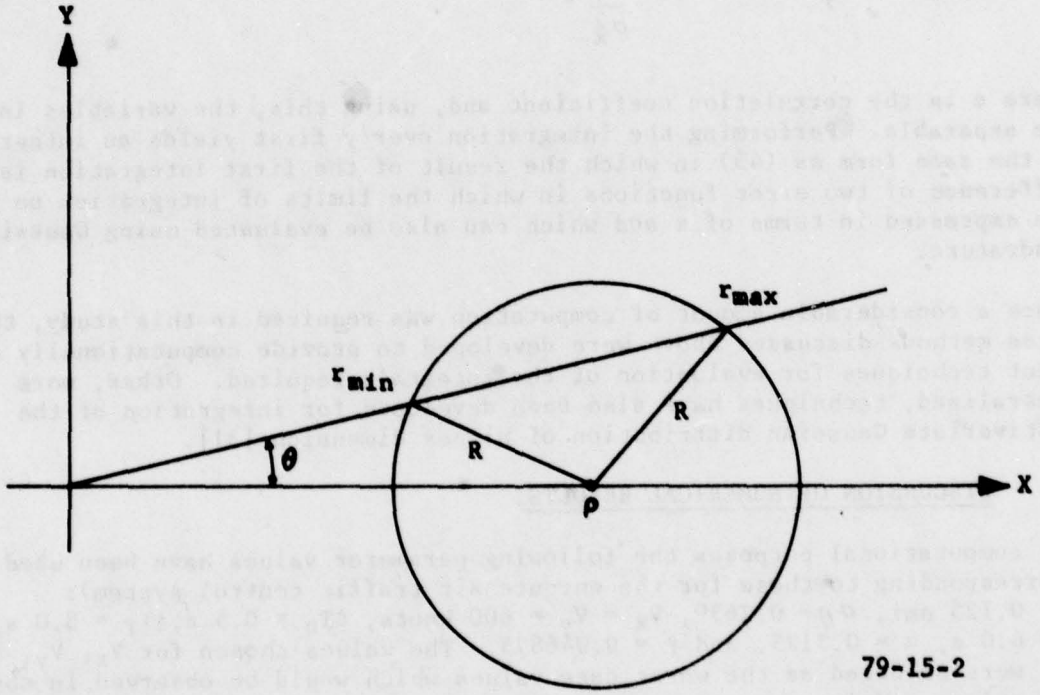

FIGURE 2. DERIVATION OF RANGE LIMITS FOR PROBABILITY CALCULATIONS

3.3 EVALUATION IN CARTESIAN COORDINATES.

The probability density function of the bivariate Gaussian distribution, f(x,y) contains terms with the product xy and so cannot be factored, but if the joint density is written as

$$f(x, y) = f(x)\, f(y/x) \tag{46}$$

then the integration can be more readily accomplished, because the conditional density function f(y/x) is Gaussian with moments [30]:

$$E(y/x) = c\,\frac{\sigma_y}{\sigma_x}\,x \tag{47}$$

$$E(y^2/x) = \sigma_y^2\,(1-c^2) + c^2\,\frac{\sigma_y^2}{\sigma_x^2}\,x^2 \tag{48}$$

where c is the correlation coefficient and, using this, the variables in (46) are separable. Performing the integration over y first yields an integral of the same form as (45) in which the result of the first integration is the difference of two error functions in which the limits of integration on y are expressed in terms of x and which can also be evaluated using Gaussian quadrature.

Since a considerable amount of computation was required in this study, the three methods discussed above were developed to provide computationally efficient techniques for evaluation of the integrals required. Other, more generalized, techniques have also been developed for integration of the multivariate Gaussian distribution of higher dimension [31].

3.4 DISCUSSION OF NUMERICAL RESULTS.

For computational purposes the following parameter values have been used (corresponding to those for the enroute air traffic control system): σ_ρ = 0.125 nmi, σ_θ = 0.263°, $V_x = V_y$ = 600 knots, ΔT_q = 0.5 s, ΔT_T = 3.0 s, T = 6.0 s, α = 0.3125, and β = 0.046875. The values chosen for V_x, V_y, and ΔT_T were selected as the worst case values which would be observed in normal situations. Using these parameter values, the contribution of timing errors in (37) is negligible, with the result that the variance is about 28.1 percent larger than the variance of the measurement error alone, and this is due mainly to the contribution of the predicted position K_p. To obtain the radius of the circle required to assure a specified level of correlation, in this case 95 percent, a numerical interpolation routine was used to find the radius as a function of the desired probability. The numerical interpolation was required because it is considerably easier to find the probability as a function of the radius, rather than vice versa. The results of these computations are given by the lower line, corresponding to a zero offset, in Figure 3. Note that the results are independent of azimuth and depend only on the distance to the sensor. To insure computational accuracy, both

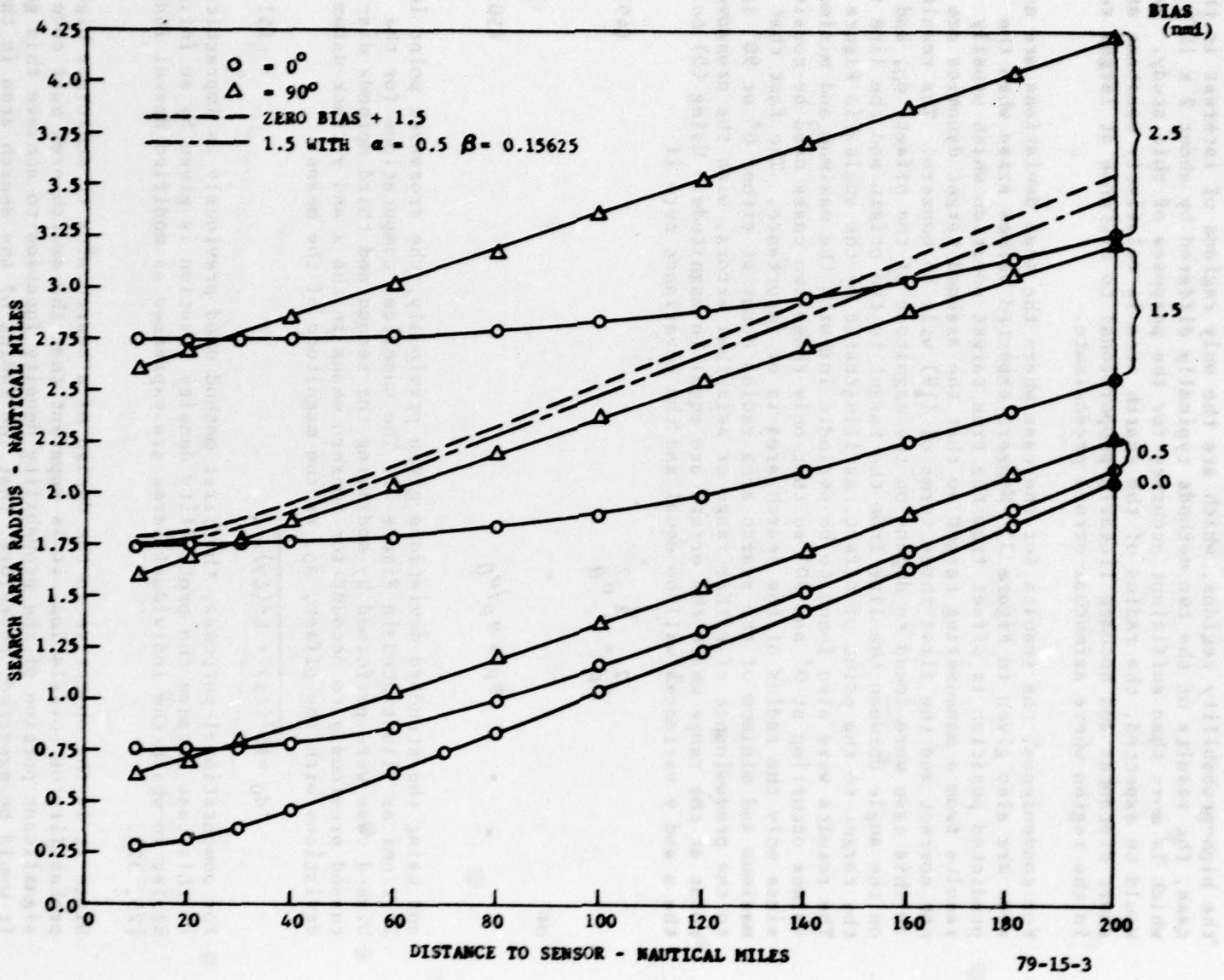

FIGURE 3. SEARCH AREA RADIUS FOR 95-PERCENT CORRELATION

methods 1 and 2 above were used to provide a check on the results. In the high-probability regions, which are the only regions of interest in this case, the results of the two methods typically differed by about 2×10^{-4}, which is more than sufficient accuracy for the purposes of this study. As would be expected, the radius of the search area is relatively constant at short distances and becomes linearly proportional to distance at larger ranges in the region where azimuthal errors predominate.

For convenience, the results for the case where the mean deviations are not zero are also given in Figure 3. Nonzero expected values arise when the predicted position is offset from the true target position which usually results from a maneuvering target so that the assumed target dynamics are not correct and the first three terms of (19) will be nonzero. The results in this case were found to depend on the magnitude of the offset, d_0, and on the angle between the line from the target to the origin and the line from the target to the point of offset, as illustrated by the angle ϕ in Figure 4. The results were also found to be periodic in ϕ with the maximum and minimum values occurring at 0° and 90° so that only these two cases need be considered, since only the radius of the search area is of importance. The fact that the maximum and minimum of the search area radius occur at either 0° or 90° is due to the predominance of either range or azimuthal errors, with the crossover point at the range where the errors are equal in magnitude. Using (5) to (7), the x and y variances will be equal and the covariance zero if

$$\sigma_\rho^2 = \rho^2 \sigma_\theta^2 \tag{49}$$

or

$$\rho = \sigma_\rho / \sigma_\theta \tag{50}$$

and using the standard deviations given previously, the crossover point is 27.2 nmi as illustrated in Figure 3. The numerical computations for the biased case were performed by modifying the second and third methods discussed previously to account for nonzero means in the x and y track datum deviations with the offset, d_0, as the magnitude of the means:

$$d_0 = \sqrt{E^2(\Delta x) + E^2(\Delta y)}. \tag{51}$$

For computational purposes, the first method used previously is impractical in this case because the probability density function is given by an infinite series in which the individual terms are expressed as modified Bessel functions [25, 32].

Since it is the objective in the design of a search area to achieve a high probability of correlation, it is apparent that the search area must cover a significant portion of the probability density function to achieve this goal. It would be expected, therefore, that the radius of the search area in the biased case would have to be sufficiently large so as to compensate for most

of the bias, and the results in Figure 3 show this to be the case; however, it is not necessary to compensate for the entire amount of the bias as shown by the results, also in Figure 3, in which 1.5 nmi was simply added to the radius required in the unbiased case. When a bias occurs, it is likely that the target is maneuvering, in which case different smoothing constants may be used. Also shown in Figure 3 are the results for the case where the bias was 1.5 nmi and the α and β smoothing constants were 0.5 and 0.15625, respectively, and these results agree fairly closely with those for the case where 1.5 nmi was added to the radius required in the unbiased case (which were obtained with different smoothing constants). For practical purposes, therefore, the radius of a circular search area required for a constant probability of correlation can be taken as the sum of the radius required in the unbiased case plus the magnitude of any bias which may be present, and this is especially true in the case where larger smoothing constants are used when a bias is detected.

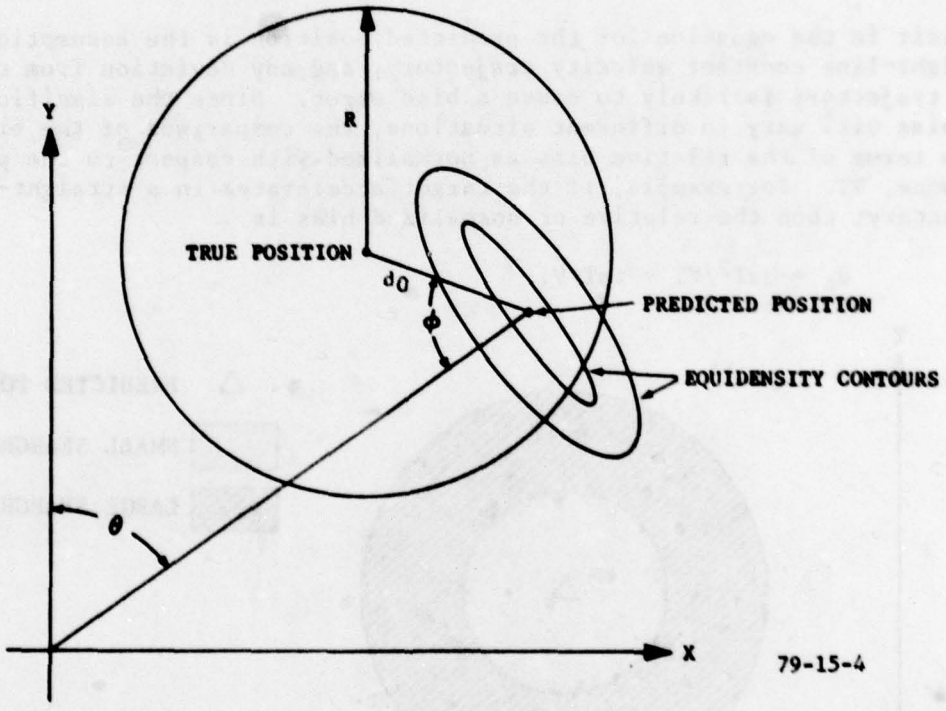

FIGURE 4. ILLUSTRATION OF OFFSET SEARCH AREA FOR NONZERO BIAS

3.5 TRACKING BIASES FOR MANEUVERING TARGETS.

It was stated previously that one of the functions of the correlation task is to choose between alternative sets of smoothing constants, and this function can be achieved by dividing the correlation region into subareas, each of which is associated with a particular set of smoothing constants. For the purposes of this study, the correlation region will be divided into large and small search areas as illustrated in Figure 5. The size of the small search area, in which smoothing constants applicable to straight-line tracks are used, is determined by the results in Figure 3 for the unbiased case, while the size of the large search area, in which smoothing constants applicable to turning tracks are used, will be taken as the sum of the radius of the small search area plus the magnitude of any bias which may be present. Therefore, in order to determine the size of the large search area it is necessary to determine the magnitude of the bias which will result from realistic maneuvers. By determining the maximum bias which can be realistically be expected to develop, it will be possible to design the large search area on a worst case basis so that correlation will be possible for all realistic maneuvers.

Implicit in the equation for the predicted position is the assumption of a straight-line constant velocity trajectory, and any deviation from this idealized trajectory is likely to cause a bias error. Since the significance of the bias will vary in different situations, the comparison of the bias will be in terms of the relative bias as normalized with respect to the prediction distance, VT. For example, if the target accelerates in a straight-line trajectory, then the relative or normalized bias is

$$d_n = \tfrac{1}{2}aT^2/VT = \tfrac{1}{2}aT/V. \qquad (52)$$

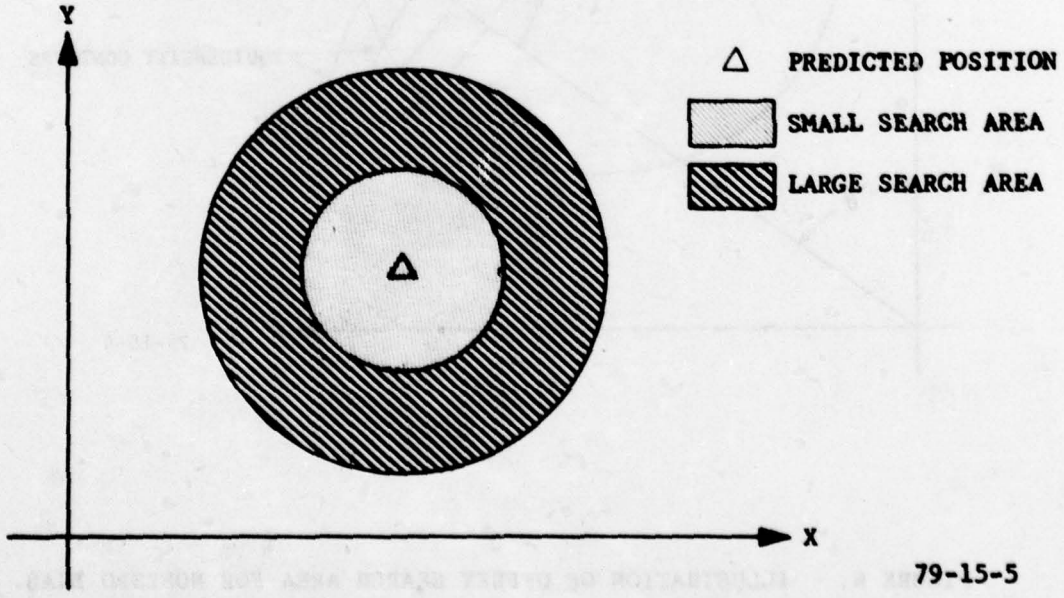

FIGURE 5. ILLUSTRATION OF LARGE AND SMALL SEARCH AREAS

Assuming worst case values of 100 knots/minute and 100 knots for acceleration and velocity, respectively, for a 6-second sampling time, the normalized bias is 0.05, but in most cases it will be less than this and negligible for practical purposes. A climbing or descending target can also introduce a bias in the predicted position. If a target is moving at a constant velocity and then begins a vertical transition at a constant vertical velocity, V_v, while maintaining the same airspeed, then the true ground speed will decrease, resulting in a normalized bias of

$$d_n = 1 - \sqrt{1 - (V_v/V)^2} \tag{53}$$

and choosing worst case values of 4,000 feet/minute and 100 knots for V_v and V, respectively, the normalized bias in this case is 0.085, which is also negligible for practical purposes.

Both of the biases just discussed are relatively small and occur in the line of the trajectory. For a turning trajectory, however, substantially larger biases can develop which are not along the straight-line projection of the velocity vector. For a target moving at a constant speed in a circular path in which the heading changes at a constant rate, ω, it can be shown, by integration of the parametric equations of motion, that the normalized bias at time T is

$$d_n = \sqrt{1 + (\sin(\omega T/2)/(\omega T/2))^2 - 2\omega T \sin(\omega T)} \tag{54}$$

which is plotted in Figure 6. The results show that the normalized bias increases with the total heading change, ωT, to a maximum of 1.26 and then asymptotically approaches one in an oscillatory manner. The reason the normalized bias approaches one is illustrated in Figure 7. As the heading change increases, with the target repeatedly traveling a circular trajectory, a point is soon reached at which the diameter of the trajectory is much less than the linear projection, hence the asymtotic value of one. Since a typical turning rate is on the order of 3° per second or less, it is apparent that a significant bias would not develop until several scans had elapsed during which no data were received for the track. If a target maneuver takes several scans, as it usually does, then the effect of tracking on the bias must also be considered.

It has been shown that of the maneuvers which have been considered, the bias observed during a turn is the largest, however, this is without considering the effect of tracking. For simplicity in analyzing the effect of tracking it would be desirable to restrict consideration to turning maneuvers. The justification for this simplifying restriction is that for nonturning maneuvers, only the constant velocity assumption used in the tracking prediction is violated, while a turn represents a violation of both the straight-line and constant velocity assumptions. In addition, a turn represents a time-varying acceleration (in Cartesian coordinates), while the other maneuvers considered represent a constant acceleration. It is concluded, therefore, that if the bias which is used to determine the size of the large search area is based on a turn, which represents a worst case situation, then if it is possible to track turning targets with this large search area size, it will also be possible to track other maneuvers which produce a smaller bias.

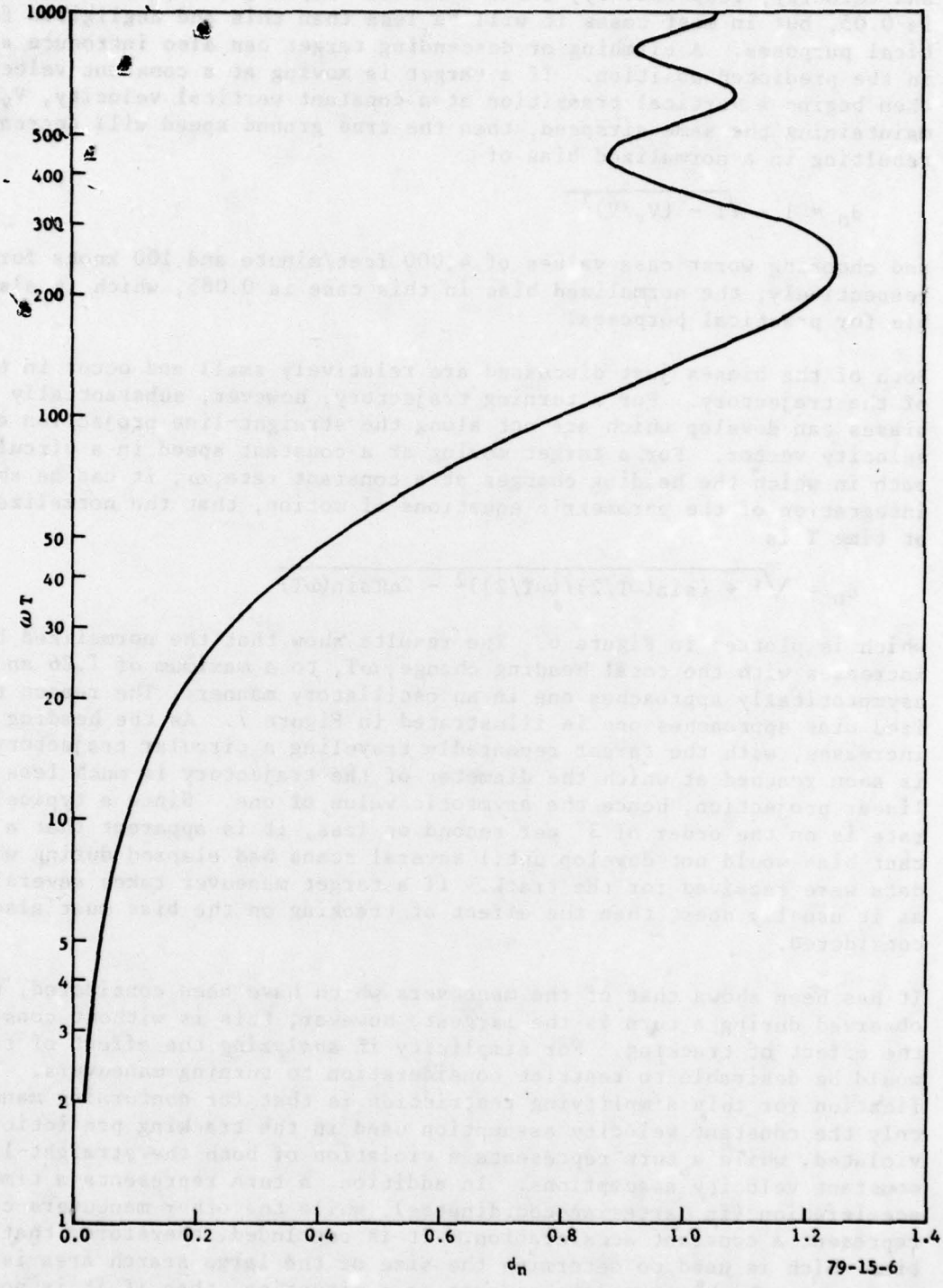

FIGURE 6. NORMALIZED POSITION BIAS FOR CIRCULAR TRAJECTORIES

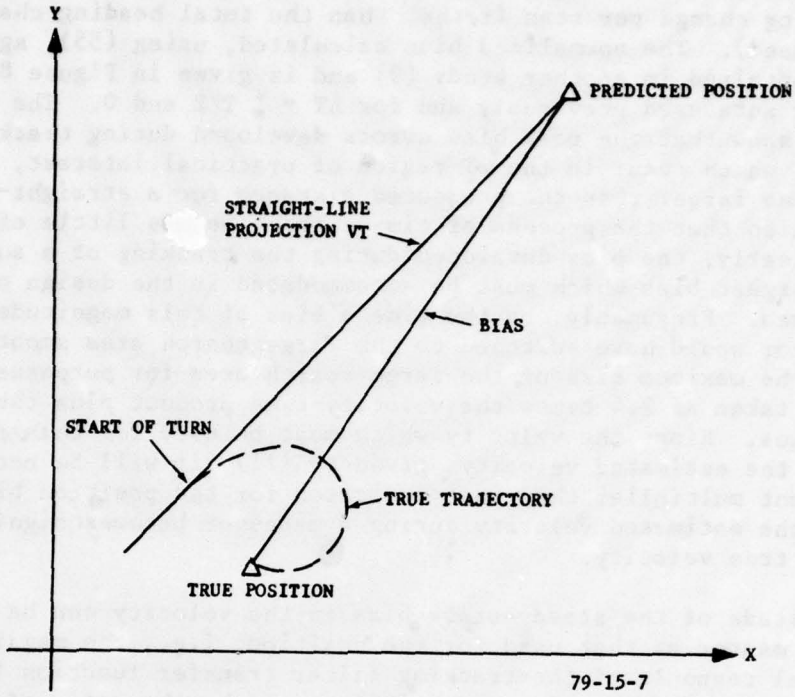

FIGURE 7. ILLUSTRATION OF BIAS FOR CIRCULAR TRAJECTORIES

Unless the tracking function is exactly able to compensate for the bias as it occurs, which is not possible, then it would be expected that the effect of the bias on each scan would be cumulative and would increase until a steady-state value had been reached. The magnitude of the steady-state bias in position has been determined by calculating the magnitude of the sinusoidal response of the tracking filter transfer function, which would correspond to a circular trajectory, and after normalization

$$d_n = \frac{4 \sin^2(\omega T/2)/\omega T}{\{[(\alpha+\beta-2-\beta\Delta T/T) + (2-\alpha+\beta\Delta T/T)\cos\omega T]^2 + [(\alpha-\beta\Delta T/T)\sin\omega T]^2\}^{1/2}} \quad (55)$$

where α and β are the smoothing constants of the tracking filter and ωT is the heading change per scan (rather than the total heading change as previously used). The normalized bias calculated, using (55), agrees with the results obtained in another study [9] and is given in Figure 8 for the two parameter sets used previously and for $\Delta T = \pm T/2$ and 0. The results in Figure 8 show that the peak bias errors developed during tracking of a maneuver, which occur in the ωT-region of practical interest, can be two to three times larger than the projected distance for a straight-line trajectory, VT, and also that the process of time-correction has little effect in this case. Clearly, the bias developed during the tracking of a sustained maneuver is the largest bias which must be accommodated in the design of the large search area. Presumably, by the time a bias of this magnitude had developed, the tracker would have switched to the large search area smoothing constants so that the maximum size of the large search area for purposes of correlation could be taken as 2.4 times the velocity-time product plus the small search area radius. Since the velocity which must be used for this purpose, however, is the estimated velocity, given by (11), it will be necessary to use a different multiplier than that indicated for the position bias in Figure 8, because the estimated velocity during a maneuver becomes significantly less than the true velocity.

The magnitude of the steady-state bias in the velocity can be determined in the same manner as that used for the position; i.e., the magnitude of the sinusoidal response of the tracking filter transfer function for velocity will be the steady-state speed. Using this approach, the ratio of the estimated speed to the true speed is

$$\frac{|\bar{V}_S|}{|\bar{V}_T|} = \frac{\beta}{\omega T} \frac{\left\{ \begin{array}{l} [(3-\alpha-\beta+\beta\Delta T/T)+(2\alpha+\beta-4-2\beta\Delta T/T)\cos\omega T+(1-\alpha+\beta\Delta T/T)\cos 2\omega T]^2 \\ +[(2\alpha+\beta-2-2\beta\Delta T/T)\sin\omega T+(1-\alpha-\beta\Delta T/T)\sin 2\omega T]^2 \end{array} \right\}^{\frac{1}{2}}}{\{[(\alpha+\beta-2-\beta\Delta T/T)+(2-\alpha+\beta\Delta T/T)\cos\omega T]^2 + [(\alpha-\beta\Delta T/T)\sin T]^2\}^{\frac{1}{2}}} \quad (56)$$

which is also plotted in Figure 8. As the results show, the bias in velocity can be significant, especially for the small search area smoothing constants given previously. To check the accuracy of this equation, a statistical simulation of the tracking algorithm was performed and the simulation results, in terms of the ratio of the estimated speed to the true speed, agreed very well with the ratio obtained using (56).

If the estimated velocity, which in practical situations is the only velocity information available, is to be used for determination of the large search area size, then in order to compensate for the velocity bias, the estimated velocity must be divided by the normalized velocity bias factor in order to obtain an estimate of the true velocity. Therefore, if the product of the filter period and the estimated velocity is to be used to calculate the maximum position bias in order to specify the size of the large search area, then this product must be multiplied by the ratio of the normalized position

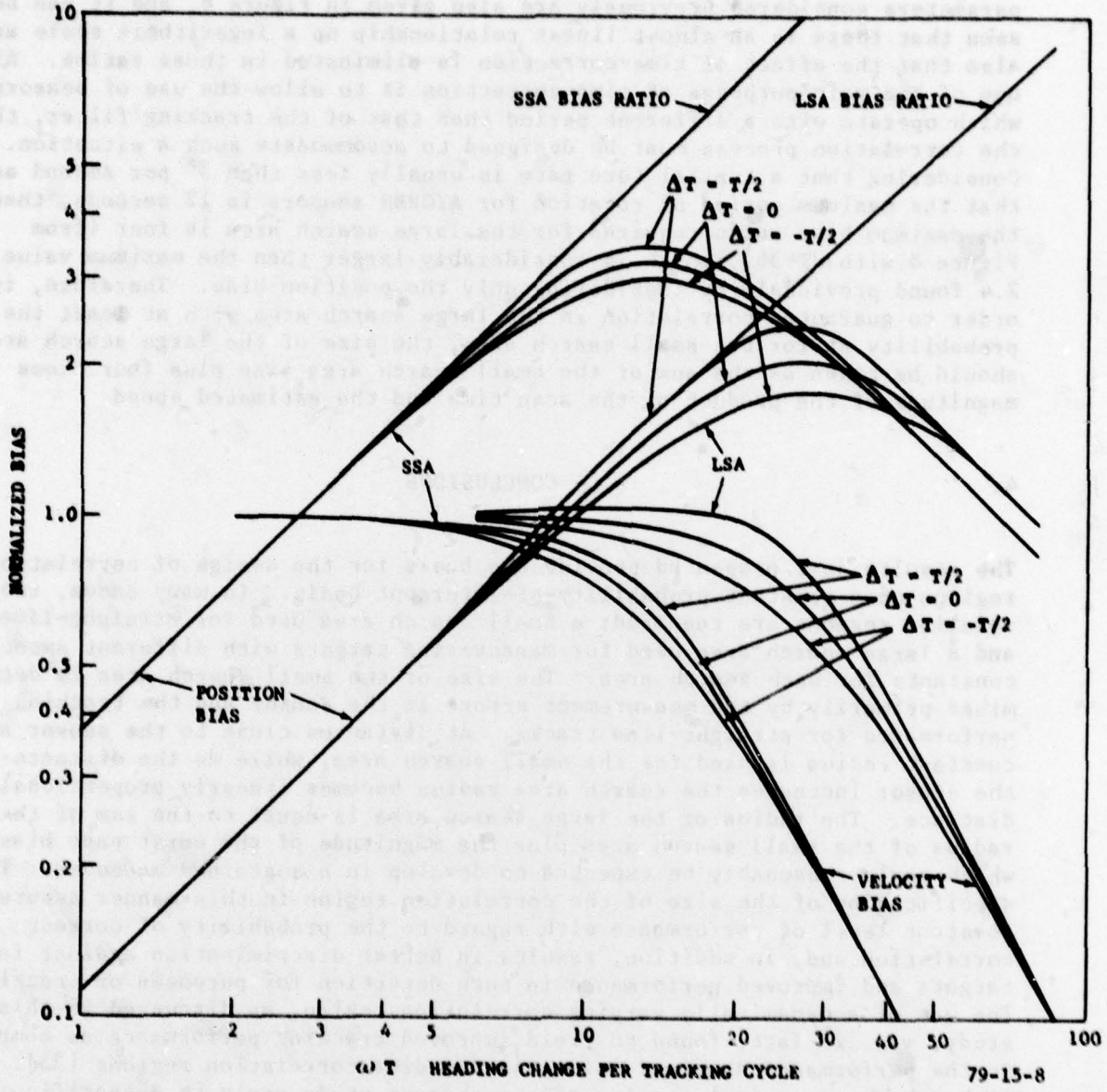

FIGURE 8. NORMALIZED POSITION AND VELOCITY BIASES DURING MANEUVERS WITH TRACKING

bias to the normalized velocity bias in order to compensate for both the position and velocity biases. The bias ratios for the two sets of smoothing parameters considered previously are also given in Figure 8, and it can be seen that there is an almost linear relationship on a logarithmic scale and also that the effect of time-correction is eliminated in these ratios. Since one of the main purposes of time-correction is to allow the use of sensors which operate with a different period than that of the tracking filter, then the correlation process must be designed to accommodate such a situation. Considering that a typical turn rate is usually less than 3° per second and that the maximum period of rotation for ATCRBS sensors is 12 seconds, then the maximum bias ratio required for the large search area is four (from Figure 8 with $\omega T=36$), which is considerably larger than the maximum value of 2.4 found previously by considering only the position bias. Therefore, in order to guarantee correlation in the large search area with at least the same probability as for the small search area, the size of the large search area should be taken as the sum of the small search area size plus four times the magnitude of the product of the scan time and the estimated speed.

4. CONCLUSIONS

The results just presented provide the basis for the design of correlation regions on a constant-probability-of-intercept basis. In many cases, two correlation regions are required: a small search area used for straight-line tracks and a large search area used for maneuvering targets with different smoothing constants for each search area. The size of the small search area is determined primarily by the measurement errors in the sensor and the tracking performance for straight-line tracks. At distances close to the sensor a constant radius is used for the small search area, while as the distance to the sensor increases the search area radius becomes linearly proportional to distance. The radius of the large search area is equal to the sum of the radius of the small search area plus the magnitude of the worst case bias which could reasonably be expected to develop in a sustained maneuver. The specification of the size of the correlation region in this manner assures a constant level of performance with regard to the probability of correct correlation and, in addition, results in better discrimination against false targets and improved performance in turn detection for purposes of tracking. The use of a dynamically varying correlation region, as discussed in this study, was, in fact, found to yield improved tracking performance as compared to the performance obtained using fixed radius correlation regions [33]. Although the numerical results of the present study apply to a specific α-β tracking filter, the technique developed could easily be applied to other tracking filters.

5. REFERENCES

1. Sittler, R. W., "An Optimal Data Association Problem in Surveillance Theory," IEEE Trans. on Military Electronics, Vol. MIL-8, pp. 125-139, April 1964.

2. Kanyuck, A. J. and Singer, R. A., "Correlation of Multiple-Site Track Data," IEEE Trans. on Aerospace and Electronic Systems, Vol. AES-6, pp. 180-187, March 1970.

3. Singer, R. A. and Kanyuck, A. J., "Computer Control of Multiple-Site Track Correlation," Automatica, Vol. 7, pp. 455-463, July 1971.

4. Singer, R. A. and Sea, R. G., "New Results in Optimizing Surveillance System Tracking and Data Correlation Performance in Dense Multitarget Environments," IEEE Trans. on Automatic Control, Vol. AC-18, pp. 571-582, December 1973.

5. Singer, R. A., Sea, R. G., and Housewright, K. B., "Derivation and Evaluation of Improved Tracking Filters for Use in Dense Multitarget Environments," IEEE Trans. on Information Theory, Vol. IT-20, pp. 423-432, July 1974.

6. Alspach, D. L., "A Gaussian Sum Approach to the Multitarget Identification-Tracking Problem," Automatica, Vol. 11, pp. 285-296, May 1975.

7. Morefield, C. L., "Application of 0-1 Integer Programming to Multitarget Tracking Problems," IEEE Trans. on Automatic Control, Vol. AC-22, pp. 302-312, June 1977.

8. Shaw, N. K. and Simolunas, A. A., "System Capability of Air Traffic Control Radar Beacon System," Proc. of the IEEE, Vol. 58, pp. 399-407, March 1970.

9. Sklansky, J., "Optimizing the Dynamic Performance of a Track-While-Scan System," RCA Review, Vol. 18, pp. 163-185, June 1957.

10. Levine, N., "A New Technique for Increasing the Flexibility of Recursive Least Squares Data Smoothing," Bell System Technical Journal, Vol. 11, pp. 821-840, May 1961.

11. Benedict, T. R. and Bordner, G. W.,"Synthesis of an Optimal Set of Radar Track-While-Scan Smoothing Equations," IRE Trans. on Automatic Control, Vol. AC-7, pp. 27-32, July 1962.

12. Simpson, H. R., "Performance Measures and Optimization Condition for a Third-Order Sampled-Data Tracker," IEEE Trans. on Automatic Control (Correspondence), Vol. AC-8, pp. 182-183, April 1963.

13. Neal, S. R., "Discussion on Parametric Relations for the α-β-γ Filter Predictor," IEEE Trans. on Automatic Control (Correspondence), Vol. AC-12, pp. 315-317, June 1967.

14. Kanyuck, A. J., "Transient Response of Tracking Filters With Randomly Interrupted Data," IEEE Trans. on Aerospace and Electronic Systems, Vol. AES-6, pp. 313-323, May 1960.

15. Singer, R. A. and Behnke, K. W., "Real-Time Tracking Filter Evaluation and Selection for Tactical Applications," IEEE Trans. on Aerospace and Electronic Systems, Vol. AES-7, pp. 100-110, January 1971.

16. Wilson, K. C., "An Optimal Control Approach to Designing Constant Gain Filters," IEEE Trans. on Aerospace and Electronic Systems, Vol. AES-8, pp. 836-842, November 1972.

17. Bhagavan, B. K. and Polge, R. J., "Performance of the g-h Filter for Tracking Maneuvering Targets," IEEE Trans. on Aerospace and Electronic Systems (Correspondence), Vol. AES-10, pp. 864-866, November 1974.

18. Schooler, C. C., "Optimal α-β Filters for Systems with Modeling Inaccuracies," IEEE Trans. on Aerospace and Electronic Systems, Vol. AES-11, pp. 1300-1306, November 1975.

19. Cantrell, B. H., Behavior of α-β Tracker for Maneuvering Targets Under Noise, False Target and Fade Conditions, Naval Research Laboratory Report 7434, NTIS No. AD748-993, August 1972.

20. Cantrell, B. H., Description of an Alpha-Beta Filter in Cartesian Coordinates, Naval Research Laboratory Report 7548, NTIS No. AD759-011, March 1973.

21. Cantrell, B H., Gain Adjustment of an Alpha-Beta Filter with Random Updates, Naval Research Laboratory Report 7647, NTIS No. AD774-087, December 1973.

22. Cantrell, B. H., Adaptive Tracking Algorithm, Naval Research Laboratory Memorandum 3037, NTIS No. AD-A011-122, April 1975.

23. Navarro, A. M., General Properties of Alpha Beta, and Alpha Beta Gamma Tracking Filters, Physics Laboratory Report PHL 1977-02, NTIS No. N77-24347, January 1977.

24. Cadzow, J. A., Discrete-Time Systems, Prentice-Hall, Englewood Cliffs, N. J., 1973.

25. Nakagami, M. "The m-Distribution-A General Formula of Intensity Distribution of Rapid Fading," in Statistical Methods in Radio-Wave Propagation edited by W. C. Hoffman, Oxford: Pergamon Press, pp. 3-36, 1960.

26. Nakagami, M. "On the Intensity Distribution and Its Application to Signal Statistics," Radio Science Journal of Research NBS, Vol. 68D, pp. 995-1003, September 1964.

27. Abramowitz, M. and Stegun, I. A., Editors; Handbook of Mathematical Functions with Formulas, Graphs, and Mathematical Tables, Washington, D.C.: Government Printing Office, 1964.

28. Sookne, D. J., "Bessel Functions of Real Argument and Integer Order," Journal of Research of the National Bureau of Standards, Vol. 77A, pp. 125-132, July-December 1973.

29. Krylov, V. I., Approximate Calculation of Integrals, New York, N. Y.: Macmillan, 1962.

30. Papoulis, A., Probability Random Variables and Stochastic Processes, New York, N. Y.: McGraw-Hill, 1965.

31. Milton, R. C., "Computer Evaluation of the Multivariate Normal Integral," Technometrics, Vol. 14, pp. 881-889, November 1972.

32. Beckmann, P., "Statistical Distribution of the Amplitude and Phase of a Multiply Scattered Field," Journal of Research of the National Bureau of Standards, Vol. 66D, pp. 231-240, May-June 1962.

33. Mullin, F. R., The Use of Dynamic Search Areas in the National Airspace System Enroute Computer Program, Federal Aviation Administration Report FAA-RD-75-77, NTIS No. AD-A012-496, May 1975.